

Improved Selectivity for Cu(II) of Methyl-Substituted Poly(pyrazolyl)-borates, $[HB(3\text{-}Mepz)_3]^-$ and $[B(3\text{-}Mepz)_4]^-$, through Steric Contact

Tsuyoshi Kitano,* Yoshiki Sohrin, Yasuo Hata, Hiroki Wada,† Takeyoshi Hori,† and Kazumasa Ueda†

Institute for Chemical Research, Kyoto University, Uji, Kyoto 611-0011

†Faculty of Technology, Kanazawa University, 2-40-20 Kodatsuno, Kanazawa 920-8667

(Received November 14, 2002)

The separation of first-series transition metal and Cd^{2+} ions has been studied by solvent extraction using methyl substituted poly(pyrazolyl)borates. These ligands did not extract all of the studied metal ions at a lower pH compared to the parent ligands, and the selectivity was high for Cu(II) and low for Fe(II), although the extracted species were A_2M complexes as well (A^-: poly(pyrazolyl)borate, M^{2+}: metal ion) for all the four ligands. An examination of the structures of the nine complexes determined the present and related ones, which were previously determined elsewhere, revealed that 3-methyl groups of the pyrazolyl rings are arrayed around a metal ion, and that the distances between the methyl groups are smaller than the sum of van der Waals radii of the methyl groups. This suggests that the interligand contact of 3-methyl groups decreases the stability of the complexes. Since the geometry in the copper complexes with these ligands is square bipyramid, the increase in steric energy caused by the interligand contact seems to be smaller than that for those complexes having similar ionic radii. Moreover, the spin state of the iron complexes with these ligands is high-spin due to interligand contact. Thus, while the interligand contact causes a general decrease in the stability of all the complexes, the effect is smallest for Cu(II) and largest for Fe(II), resulting in a unique selectivity.

Recently, poly(pyrazolyl)borates have been employed for various purposes. Many researchers have utilized them for mimicking metalloenzyme systems[1–5] and to develop a novel catalytic reaction center. In particular, because bulky substituents at the 3- and/or 5-positions of the pyrazolyl ring provide a unique steric coordination control, some investigators have developed new ligands having bulkier substituents.[6–11] Although various transition-metal ions, including the second and third series, were studied as a metal center of the poly(pyrazolyl)borate complexes,[12–23] there have only been a few investigations concerning the influence of substituents on the selectivity of the ligands for transition-metal ions.

In a previous paper, we reported on the solvent extraction of first-series transition-metal ions and Cd(II) with $[HB(pz)_3]^-$ and $[B(pz)_4]^-$. Because $[HB(pz)_3]^-$ coordinated to a metal ion in a tripodal tridentate fashion, it extracted all of the studied metal ions from an acidic aqueous solution ($pH < 2.1$). On the other hand, $[B(pz)_4]^-$ did not extract large metal ions, such as Mn(II) and Cd(II), around lower pH compared to $[HB(pz)_3]^-$. Also, the extraction constant of $[B(pz)_4]^-$ for Cu(II) was low and did not conform to the order of the Irving-Williams series. Because of the intraligand contact between pyrazolyl rings, $[B(pz)_4]^-$ accompanied substantial steric energy increases in coordination to Mn(II), Cu(II) and Cd(II), decreasing the stability of the complexes, resulting in unique selectivity.[24]

Here, we report on the results of the solvent extraction of Mn(II), Fe(II), Co(II), Ni(II), Cu(II), Zn(II) and Cd(II) with tripodal poly(pyrazolyl)borates that contain methyl substituted pyrazolyl rings, namely, $[HB(3\text{-}Mepz)_3]^-$ and $[B(3\text{-}Mepz)_4]^-$. $[HB(3\text{-}Mepz)_3]^-$ and $[B(3\text{-}Mepz)_4]^-$ were found to be improved in the separability for these metal ions compared with $[HB(pz)_3]^-$ and $[B(pz)_4]^-$, respectively. The extraction reaction for a small metal ion, such as Ni(II), with $[HB(3\text{-}Mepz)_3]^-$ and $[B(3\text{-}Mepz)_4]^-$ was slow. To explore the origin of the selectivity, X-ray crystal structures of the extracted species, $[HB(3\text{-}Mepz)_3]_2Mn$ (**1**), $[HB(3\text{-}Mepz)_3]_2Co$ (**2**), $[HB(3\text{-}Mepz)_3]_2Zn$ (**3**), $[HB(3\text{-}Mepz)_3]_2Cd$ (**4**), $[B(3\text{-}Mepz)_4]_2Mn$ (**5**), $[B(3\text{-}Mepz)_4]_2Fe$ (**6**), $[B(3\text{-}Mepz)_4]_2Co$ (**7**), $[B(3\text{-}Mepz)_4]_2Ni$ (**8**) and $[B(3\text{-}Mepz)_4]_2Zn$ (**9**), were determined. The X-ray structures of the 28 A_2M complexes of $[HB(3\text{-}Mepz)_3]^-$, $[B(3\text{-}Mepz)_4]^-$, $[HB(pz)_3]^-$ and $[B(pz)_4]^-$ with Mn(II), Fe(II), Co(II), Ni(II), Cu(II), Zn(II) and Cd(II) are compared precisely, and the steric factors controlling the selectivity are discussed.

Results

Acid Dissociation and Distribution Constants of the Ligands. $[HB(3\text{-}Mepz)_3]^-$ and $[B(3\text{-}Mepz)_4]^-$ are polyacidic bases. The acid-dissociation constants are defined as

$$K_{a1} = [H^+][HA]/[H_2A^+], \quad (1)$$

$$K_{a2} = [H^+][A^-]/[HA], \quad (2)$$

where the brackets represent the molar concentration in aqueous solution and A^- stands for the poly(pyrazolyl)borates. The distribution constant of the ligand is defined as

$$P_{HA} = [HA]_o/[HA], \quad (3)$$

where the subscript o denotes the species in the organic phase.

Published on the web July 15, 2003; DOI 10.1246/bcsj.76.1365

Table 1. Acid Dissociation and Partition Constants of the Poly(pyrazolyl)borates Used

	pK_{a1}	pK_{a2}	$\log P_{HA}$
$[HB(pz)_3]^-$ a)	3.40	7.39	0.23
$[B(pz)_4]^-$ a)	2.58	6.08	0.98
$[HB(3\text{-}Mepz)_3]^-$	3.12	9.81	−0.12
$[B(3\text{-}Mepz)_4]^-$	2.35	9.75	0.97

a) Data taken from Ref. 24.

The logarithm of the distribution ratio of the ligand ($\log D_{HA}$) between the aqueous and chloroform phases was plotted as a function of the pH,

$$D_{HA} = [HA]_o/([H_2A^+] + [HA] + [A^-]) = P_{HA}/([H^+]/K_{a1} + 1 + K_{a2}/[H^+]). \quad (4)$$

The plot was analyzed by a non-linear least-squares method and the distribution and acid dissociation constants were obtained. These ligands were rather quickly hydrolyzed into 3-methylpyrazole and boric acid in aqueous solution. In a distribution experiment, the ligand concentrations in the organic phase decreased with an increase in the shaking time (t min). To remove the influence of hydrolysis, $\log[HA]_o$ was plotted against t. The value at $t = 0$ was obtained by extrapolation and used for plots of $\log D_{HA}$ vs pH. The decomposition rate was highest around pH 3–9 for $[HB(3\text{-}Mepz)_3]^-$ and 2–9 for $[B(3\text{-}Mepz)_4]^-$. pK_{a1}, pK_{a2} and $\log P_{HA}$ for $[HB(3\text{-}Mepz)_3]^-$ and $[B(3\text{-}Mepz)_4]^-$ are listed in Table 1 and compared with those for $[HB(pz)_3]^-$ and $[B(pz)_4]^-$.

Extraction of First-Series Transition-Metal Ions and Cd(II). As shown in Fig. 1, the percentage extraction of the metal ions (*%E*) did not reach the maximum within 400 min of shaking for Co(II), Ni(II), Zn(II) and Cd(II). The *%E* of Cu(II) reached the maximum within 200 min with $[HB(3\text{-}Mepz)_3]^-$ and 100 min with $[B(3\text{-}Mepz)_4]^-$. The *%E* for Mn(II) and Fe(II) scattered, probably because of oxidation of the metal ions. Figure 2 shows the relationship between *%E* and the pH of the aqueous phase. Ten min of shaking was adopted for a comparison with $[HB(pz)_3]^-$ and $[B(pz)_4]^-$, although they were not sufficient for equilibrium. The *%E* value was independent of the metal-ion concentration of 3×10^{-5}–3×10^{-3} M. All of the studied metal ions were quantitatively extracted into the chloroform phase. The percentage recovery decreased slightly at a high pH, which may be attributed to oxidation and hydrolysis of metal ions and the decomposition of the ligands. It should be noted that $[HB(3\text{-}Mepz)_3]^-$ and $[B(3\text{-}Mepz)_4]^-$ did not extract all of the studied metal ions at a lower pH compared to $[HB(pz)_3]^-$ and $[B(pz)_4]^-$, respectively. $[HB(3\text{-}Mepz)_3]^-$ extracted all of the studied metal ions at a lower pH compared to $[B(3\text{-}Mepz)_4]^-$.

In order to elucidate the extracted species for Cu(II), the logarithm of the distribution ratio for Cu(II) ($\log D$) was measured at equilibrium,

$$D = C_{M,o}/C_M, \quad (5)$$

where C_M signifies the analytical molar concentration of the metal ion (M^{2+}). The overall extraction equilibrium and extraction constant (K_{ex}) of M^{2+} are described as follows:

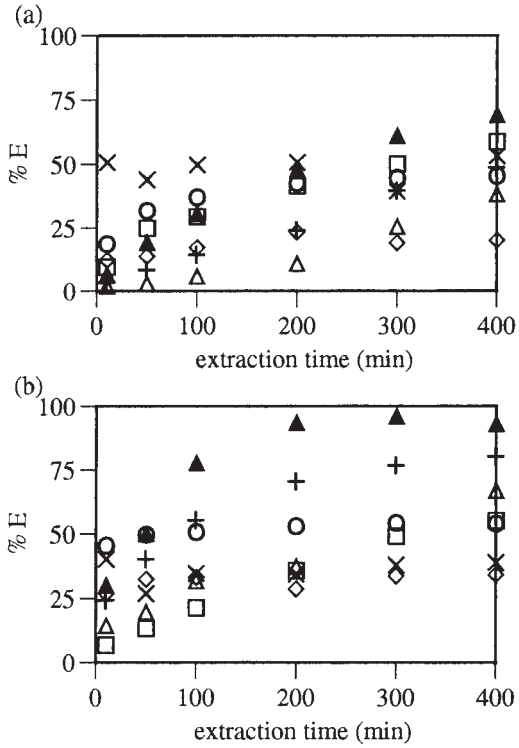

Fig. 1. Effect of extraction time on the percentage extraction of metal ions. Aqueous phase: 1×10^{-2} M KA, 1×10^{-2} M buffer, 1×10^{-4} M M^{2+} (10 mL). Organic phase: chloroform (10 mL). Key: ◇, Mn(II); ×, Fe(II); △, Co(II); +, Ni(II); ○, Cu(II); ▲, Zn(II); □, Cd(II). (a) $K[HB(3\text{-}Mepz)_3]$, pH was adjusted to 3.52 for Mn(II), 2.77 for Fe(II), 1.76 for Co(II), 1.76 for Ni(II), 0.84 for Cu(II), 1.60 for Zn(II), 1.61 for Cd(II); (b) $K[B(3\text{-}Mepz)_4]$, pH was adjusted to 4.75 for Mn(II), 3.70 for Fe(II), 2.62 for Co(II), 2.62 for Ni(II), 0.82 for Cu(II), 2.13 for Zn(II), 1.89 for Cd(II).

$$M^{2+} + 2\ HA_o \rightleftarrows A_2M_o + 2\ H^+, \quad (6)$$

$$K_{ex} = [A_2M]_o[H^+]^2/[M^{2+}][HA]_o^2, \quad (7)$$

$$\log K_{ex} = \log D + 2\log[H^+] - 2\log[HA]_o. \quad (8)$$

To analyze the extraction data graphically, the protonation and distribution of the ligands must be taken into consideration. $[HA]_o$ is expressed as

$$[HA]_o = C_{HA}/\alpha, \quad (9)$$

$$\alpha = 1 + \{[H^+]/K_{a1} + 1 + K_{a2}/[H^+]\}/P_{HA}, \quad (10)$$

where C_{HA} means the initial concentration of the ligand in the aqueous phase. The substitution of Eqs. 9 into 8 and a rearrangement results in

$$\log D - 2\log C_{HA} + 2\log\alpha = 2\ pH + \log K_{ex}. \quad (11)$$

We investigated the dependence of $\log D - 2(\log C_{HA} - \log\alpha)$ on the pH or $\log D - 2(pH - \log\alpha)$ on $\log C_{HA}$ for the extraction of Cu(II) with each ligand. The plots gave straight lines with slopes close to 2, $\log D$ was independent of C_M. These results confirm the validity of Eq. 6. The $\log K_{ex}$ values, obtained from the plots by a linear-squares fit, were 6.6 for

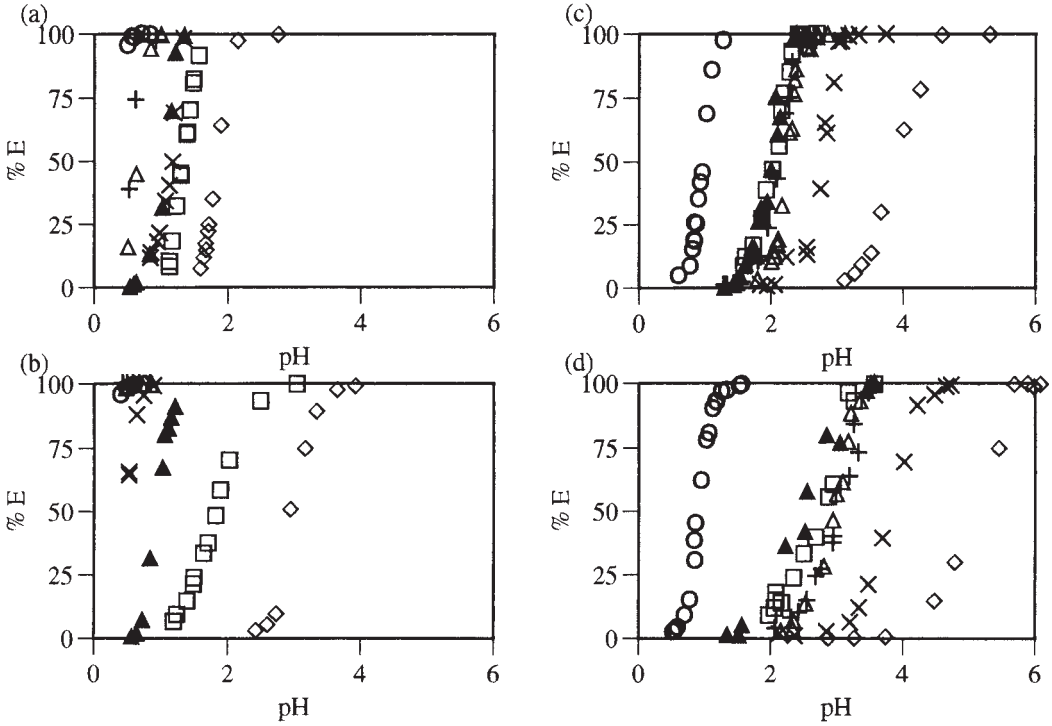

Fig. 2. Effect of pH on the percentage extraction of metal ions. Aqueous phase: 1×10^{-2} M KA, 1×10^{-2} M buffer, 1×10^{-4} M M^{2+} (10 mL). Organic phase: chloroform (10 mL). The extraction time was 10 min. Key: ◇, Mn(II); ×, Fe(II); △, Co(II); +, Ni(II); ○, Cu(II); ▲, Zn(II); □, Cd(II). (a) K[HB(pz)$_3$]; (b) K[B(pz)$_4$]; (c) K[HB(3-Mepz)$_3$]; (d) K[B(3-Mepz)$_4$]. (a), (b) Data taken from Ref. 24.

[HB(3-Mepz)$_3$]$^-$ and 3.4 for [B(3-Mepz)$_4$]$^-$.

Syntheses of the Complexes. The pH of the aqueous solution was adjusted to produce complexes according to

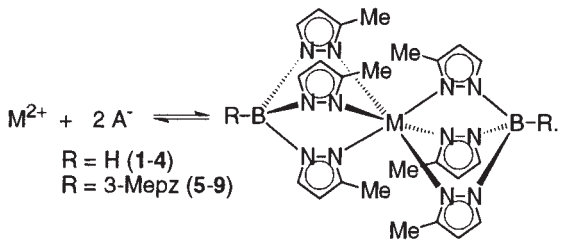

(12)

These complexes were obtained as precipitates and dissolved into chloroform, dichloromethane and benzene, and were stable in air.

Structures of the Complexes. There are two crystallographically independent molecules within a unit cell of complexes **1**–**4**. The distances between the metal and donor atoms are slightly different between the independent molecules. For **1**–**9**, each molecule is monomeric with no short intermolecular contacts. The metal atoms sit on a center of inversion. Both ligands are tridentate and the geometry about the metal atoms is a trigonally distorted octahedron. Selected bond distances and angles of **1**–**9** are shown in Tables 2–4. Figures 3 and 4 show ORTEP drawings of one of the molecules of **1** and of **5**, respectively. The structures of **2**–**4** are similar to that of **1** and the structures of **6**–**9** are similar to that of **5**. In complexes **5**–**9**, the non-coordinated pyrazolyl rings stand out in the opposite direction to the metal atoms.

The mean dimensions of the chelate rings for the studied

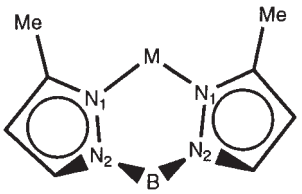

Scheme 1.

and related complexes with [HB(3-Mepz)$_3$]$^-$ and [B(3-Mepz)$_4$]$^-$ are summarized in Tables 5 and 6; the labeling of the atoms is given in Scheme 1. Tables 5 and 6 show that the average M–N1 distances are nearly equal to the sum of Shannon's ionic radii.[29] The radius of the nitrogen atom is taken as 1.32 Å for the four-coordinate N^{3-}. The radius of the metal ions of six-coordination is 0.97 Å for Mn(II) (high-spin), 0.92 Å for Fe(II) (high-spin), 0.88 Å for Co(II) (high-spin), 0.83 Å for Ni(II), 0.87 Å for Cu(II), 0.88 Å for Zn(II) and 1.09 Å for Cd(II); the M–N bond length is 2.29 Å for Mn–N, 2.24 Å for Fe–N, 2.20 Å for Co–N, 2.15 Å for Ni–N, 2.19 Å for Cu–N, 2.20 Å for Zn–N and 2.41 Å for Cd–N.

Discussion

Extraction of Transition Metal Ions. The extraction of transition-metal ions with [HB(3-Mepz)$_3$]$^-$ and [B(3-Mepz)$_4$]$^-$ was a rather slow process, especially for Co(II), Ni(II), Zn(II) and Cd(II). The extracted species were not determined by equilibrium analysis. However, the extracted species of Cu(II) with [HB(3-Mepz)$_3$]$^-$ and [B(3-Mepz)$_4$]$^-$ at

Table 2. Selected Bond Distances (Å) and Bond Angles (deg) for $[HB(3\text{-}Mepz)_3]_2Mn$ (**1**) and $[HB(3\text{-}Mepz)_3]_2Co$ (**2**)

	M = Mn (**1**)	M = Co (**2**)		M = Mn (**1**)	M = Co (**2**)
	Bond Distances			Bond Distances	
M(1)–N(1)	2.256(3)	2.151(4)	M(2)–N(7)	2.264(3)	2.155(4)
M(1)–N(3)	2.268(3)	2.156(3)	M(2)–N(9)	2.259(3)	2.166(4)
M(1)–N(5)	2.254(3)	2.153(4)	M(2)–N(11)	2.266(3)	2.163(4)
	Bond Angles			Bond Angles	
N(1)–M(1)–N(3)	84.6(1)	86.4(1)	N(7)–M(2)–N(9)	84.5(1)	86.7(1)
N(1)–M(1)–N(5)	84.53(10)	86.8(1)	N(7)–M(2)–N(11)	84.2(1)	86.4(1)
N(3)–M(1)–N(5)	84.8(1)	86.5(1)	N(9)–M(2)–N(11)	84.1(1)	86.5(2)
M(1)–N(1)–N(2)	116.0(2)	116.7(3)	M(2)–N(7)–N(8)	115.9(2)	117.0(3)
M(1)–N(3)–N(4)	116.3(2)	116.3(3)	M(2)–N(9)–N(10)	116.8(2)	115.6(3)
M(1)–N(5)–N(6)	116.0(2)	116.3(3)	M(2)–N(11)–N(12)	116.4(2)	116.2(3)
N(1)–N(2)–B(1)	121.9(2)	120.7(4)	N(7)–N(8)–B(2)	122.5(3)	120.2(3)
N(3)–N(4)–B(1)	121.4(2)	121.0(3)	N(9)–N(10)–B(2)	121.6(3)	121.8(4)
N(5)–N(6)–B(1)	121.9(2)	120.6(4)	N(11)–N(12)–B(2)	121.7(3)	120.6(4)

Table 3. Selected Bond Distances (Å) and Bond Angles (deg) for $[HB(3\text{-}Mepz)_3]_2Zn$ (**3**) and $[HB(3\text{-}Mepz)_3]_2Cd$ (**4**)

	M = Zn (**3**)	M = Cd (**4**)		M = Zn (**3**)	M = Cd (**4**)
	Bond Distances			Bond Distances	
M(1)–N(1)	2.184(2)	2.336(4)	M(2)–N(7)	2.184(3)	2.351(4)
M(1)–N(3)	2.184(2)	2.325(4)	M(2)–N(9)	2.189(2)	2.349(4)
M(1)–N(5)	2.179(2)	2.356(4)	M(2)–N(11)	2.187(2)	2.344(4)
	Bond Angles			Bond Angles	
N(1)–M(1)–N(3)	86.39(9)	82.6(2)	N(7)–M(2)–N(9)	86.14(9)	82.5(2)
N(1)–M(1)–N(5)	86.42(9)	83.1(1)	N(7)–M(2)–N(11)	86.20(9)	82.7(2)
N(3)–M(1)–N(5)	86.56(9)	83.4(1)	N(9)–M(2)–N(11)	85.98(9)	82.4(2)
M(1)–N(1)–N(2)	115.8(2)	116.1(3)	M(2)–N(7)–N(8)	116.5(2)	115.7(3)
M(1)–N(3)–N(4)	115.5(2)	116.4(3)	M(2)–N(9)–N(10)	116.1(2)	116.6(3)
M(1)–N(5)–N(6)	116.6(2)	115.9(3)	M(2)–N(11)–N(12)	116.0(2)	116.3(3)
N(1)–N(2)–B(1)	121.6(2)	122.2(4)	N(7)–N(8)–B(2)	121.4(2)	123.2(4)
N(3)–N(4)–B(1)	121.5(2)	122.2(4)	N(9)–N(10)–B(2)	121.7(2)	122.7(4)
N(5)–N(6)–B(1)	120.6(2)	121.9(4)	N(11)–N(12)–B(2)	122.2(2)	122.0(4)

Table 4. Selected Bond Distances (Å) and Bond Angles (deg) for $[B(3\text{-}Mepz)_4]_2Mn$ (**5**), $[B(3\text{-}Mepz)_4]_2Fe$ (**6**), $[B(3\text{-}Mepz)_4]_2Co$ (**7**), $[B(3\text{-}Mepz)_4]_2Ni$ (**8**) and $[B(3\text{-}Mepz)_4]_2Zn$ (**9**)

	M = Mn (**5**)	M = Fe (**6**)	M = Co (**7**)	M = Ni (**8**)	M = Zn (**9**)
			Bond Distances		
M(1)–N(1)	2.273(2)	2.199(3)	2.134(3)	2.135(2)	2.207(2)
M(1)–N(3)	2.247(3)	2.159(3)	2.172(3)	2.097(2)	2.148(2)
M(1)–N(5)	2.223(2)	2.170(3)	2.128(3)	2.099(2)	2.169(3)
			Bond Angles		
N(1)–M(1)–N(3)	84.51(9)	86.46(10)	86.50(9)	87.73(8)	86.39(9)
N(1)–M(1)–N(5)	84.46(9)	86.33(9)	85.9(1)	87.39(8)	86.23(9)
N(3)–M(1)–N(5)	83.24(10)	85.3(1)	86.67(10)	87.19(8)	85.31(9)
M(1)–N(1)–N(2)	120.0(2)	119.6(2)	116.3(2)	119.6(2)	119.4(2)
M(1)–N(3)–N(4)	114.9(2)	115.5(2)	120.0(2)	115.6(1)	115.8(2)
M(1)–N(5)–N(6)	116.3(2)	115.3(2)	115.8(2)	116.0(1)	115.3(2)
N(1)–N(2)–B(1)	117.2(2)	116.6(2)	121.2(2)	116.6(2)	116.6(2)
N(3)–N(4)–B(1)	122.5(2)	122.8(2)	116.3(2)	122.1(2)	122.9(2)
N(5)–N(6)–B(1)	123.1(2)	121.8(2)	122.5(2)	121.3(2)	121.8(2)

equilibrium were proved to be A_2M based on a slope analysis. A_2M complexes of all the metal ions were readily prepared for X-ray crystallography. Thus, it is very likely that the extracted species are A_2M, similarly to those with $[HB(pz)_3]^-$ and $[B(pz)_4]^-$.

When the shaking time was 10 min, all of the studied metal ions were not extracted with $[HB(3\text{-}Mepz)_3]^-$ and $[B(3\text{-}Mepz)_4]^-$ at a lower pH compared to $[HB(pz)_3]^-$ and $[B(pz)_4]^-$, respectively. Although the system with the methyl-substituted ligands was not in equilibrium, their shaking time was adopted consistently with that of the parent ligands, allowing for the decomposition of the ligands. The difference

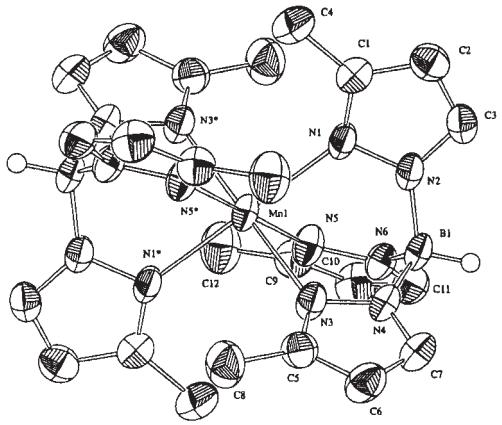

Fig. 3. ORTEP view of $[HB(3\text{-}Mepz)_3]_2Mn$ (**1**) (50% probability). Hydrogen atoms are omitted for clarity except the hydrogen atoms bonded to the boron atoms.

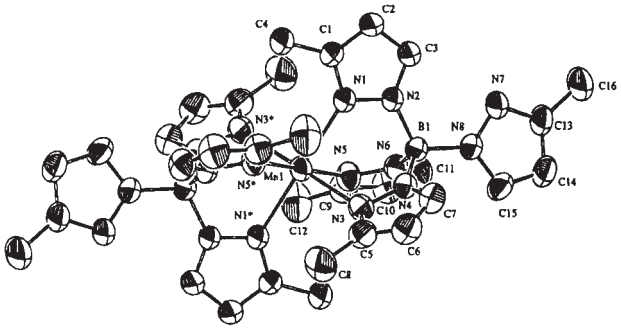

Fig. 4. ORTEP view of $[B(3\text{-}Mepz)_4]_2Mn$ (**5**) (50% probability). Hydrogen atoms are omitted for clarity.

in the extraction pH between the methyl-substituted ligands and the parent ligands was small for Cu(II), and especially large for Fe(II). This tendency did not change even though the shaking time was prolonged. Thus, the selectivity is mainly governed by thermodynamic factors, while it may be affected by kinetic factors.

K_{ex} is represented as

$$K_{ex} = P_{A2M}\beta_{A2M}{K_{a2}}^2/{P_{HA}}^2, \quad (13)$$

where P_{A2M} is the distribution constant and β_{A2M} is the stability constant for the A_2M complex. The $\log K_{ex}$ values of Cu(II) are 9.6, 6.9, 6.6 and 3.4 for $[HB(pz)_3]^-$,[24] $[B(pz)_4]^-$,[24] $[HB(3\text{-}Mepz)_3]^-$ and $[B(3\text{-}Mepz)_4]^-$, respectively. The $\log P_{HA}$ values for $[HB(pz)_3]^-$ and $[HB(3\text{-}Mepz)_3]^-$ are similar, and the K_{a2} value for $[HB(3\text{-}Mepz)_3]^-$ is smaller than that for $[HB(pz)_3]^-$ (Table 1). Similarly, the $\log P_{HA}$ values are the same for $[B(pz)_4]^-$ and $[B(3\text{-}Mepz)_4]^-$, and the K_{a2} value for $[B(3\text{-}Mepz)_4]^-$ is smaller than that for $[B(pz)_4]^-$. Thus, one of the origins of the decrease in $\log K_{ex}$ values for $[HB(3\text{-}Mepz)_3]^-$ and $[B(3\text{-}Mepz)_4]^-$ is attributable to a decrease in K_{a2}. However, the change in the selectivity is mainly controlled by the change in β_{A2M}, which is governed by steric factors. An examination of the structure of the extracted species is essential in order to elucidate the steric factors. Thus, the extracted species were synthesized and their structures were determined by X-ray crystallography.

Steric Effect of Methyl Groups in $[HB(3\text{-}Mepz)_3]^-$ and $[B(3\text{-}Mepz)_4]^-$ Complexes. Since ^1H NMR data show that the pyrazolyl rings of $[HB(3\text{-}Mepz)_3]_2Zn$ (**3**) and $[HB(3\text{-}Mepz)_3]_2Cd$ (**4**) are all equivalent, the two ligands coordinate to the metal ion in a trigonally tridentate fashion in $CDCl_3$. It was reported that the ^1H NMR data of $[B(3\text{-}Mepz)_4]_2Cd$ (**14**)

Table 5. Mean Dimensions (Å or deg) of Chelate Rings in $[HB(3\text{-}Mepz)_3]_2Mn$ (**1**), $[HB(3\text{-}Mepz)_3]_2Fe$ (**10**), $[HB(3\text{-}Mepz)_3]_2Co$ (**2**), $[HB(3\text{-}Mepz)_3]_2Ni$ (**11**), $[HB(3\text{-}Mepz)_3]_2Cu$ (**12**), $[HB(3\text{-}Mepz)_3]_2Zn$ (**3**) and $[HB(3\text{-}Mepz)_3]_2Cd$ (**4**)

	1	**10**[a)]	**2**	**11**[b)]	**12**[c)]	**3**	**4**
M–N1	2.26(1)	2.20(1)	2.16(1)	2.10(1)	2.17(15)	2.18(1)	2.34(1)
N1–M–N1	84.5(0.3)	86.4(0.1)	86.6(0.1)	88.1(0.2)	86.8(0.8)	86.3(0.2)	82.8(0.3)
M–N1–N2	116.2(0.3)	115.9(0.4)	116.4(0.5)	117.0(0.1)	115.7(2.1)	116.1(0.4)	116.2(0.3)
N1–N2–B	121.8(0.3)	121.6(0.5)	120.8(0.5)	120.5(0.1)	121.2(0.7)	121.5(0.4)	122.4(0.4)
N2–B–N2	109.9(0.3)	109.1(0.6)	109.4(0.3)	108.0(0.4)	109.3(0.7)	109.2(0.4)	110.5(0.8)
N1···N1 (intraligand)	3.04(1)	3.02(1)	2.96(1)	2.92(1)	2.98(10)	2.99(1)	3.10(1)
N1···N1 (interligand)	3.35(1)	3.21(1)	3.14(1)	3.02(1)	3.15(11)	3.19(1)	3.52(1)
M···B	3.26(1)	3.22(1)	3.17(1)	3.15(1)	3.16(1)	3.19(1)	3.32(1)

a) Data taken from Ref. 25. b) Data taken from Ref. 26. c) Data taken from Ref. 27.

Table 6. Mean Dimensions (Å or deg) of Chelate Rings in $[B(3\text{-}Mepz)_4]_2Mn$ (**5**), $[B(3\text{-}Mepz)_4]_2Fe$ (**6**), $[B(3\text{-}Mepz)_4]_2Co$ (**7**), $[B(3\text{-}Mepz)_4]_2Ni$ (**8**), $[B(3\text{-}Mepz)_4]_2Cu$ (**13**), $[B(3\text{-}Mepz)_4]_2Zn$ (**9**) and $[B(3\text{-}Mepz)_4]_2Cd$ (**14**)

	5	**6**	**7**	**8**	**13**[a)]	**9**	**14**[b)]
M–N1	2.25(2)	2.18(2)	2.15(2)	2.11(2)	2.15(15)	2.18(2)	2.35(3)
N1–M–N1	84.1(0.6)	86.0(0.5)	86.4(0.3)	87.4(0.2)	86.6(0.4)	86.0(0.5)	81.9(0.6)
M–N1–N2	117.1(2.2)	116.8(2.0)	117.3(1.8)	117.1(1.8)	116.8(0.1)	116.8(1.8)	116.1(2.0)
N1–N2–B	120.9(2.6)	120.4(2.7)	120.0(2.6)	119.9(2.4)	120.1(3.6)	120.4(2.7)	120.7(2.2)
N2–B–N2	109.2(1.4)	109.1(1.2)	108.9(1.1)	108.6(1.0)	109.1(0.2)	109.0(1.3)	109.8(0.9)
N1···N1 (intraligand)	3.01(3)	2.97(2)	2.94(2)	2.92(2)	2.95(10)	2.97(3)	3.07(3)
N1···N1 (interligand)	3.34(1)	3.18(1)	3.13(1)	3.05(1)	3.14(12)	3.18(1)	3.54(2)
M···B	3.28(1)	3.20(1)	3.19(1)	3.15(1)	3.18(1)	3.20(1)	3.33(1)

a) Data taken from Ref. 27. b) Data taken from Ref. 28.

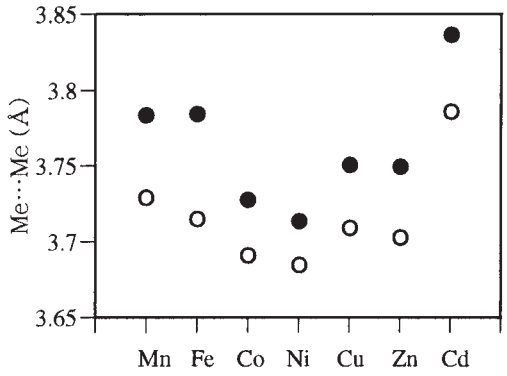

Fig. 5. Distances between the 3-methyl groups of the pyrazolyl rings of A_2M complexes. ●, $[HB(3\text{-}Mepz)_3]^-$ complexes; ○, $[B(3\text{-}Mepz)_4]^-$ complexes.

show a 3/1 ratio of the resonances at ambient temperature.[28] Only one kind of pyrazolyl ring of $[B(3\text{-}Mepz)_4]_2Zn$ (**9**) was observed with ^1H NMR, because the exchange of the coordinated and non-coordinated pyrazolyl rings in **9** was fast on the NMR time scale at ambient temperature. The rate of ligand exchange of the Zn(II) complex is generally faster than that of the Cd(II) complex.[30,31] These facts suggest that the solution structures of the studied complexes are similar to the structures in the solid state. This is probably true for the other complexes, although it was not observed whether or not their solution structures are identical with the structures in the solid state, because of their paramagnetism.

The methyl groups on the 3-position of the pyrazolyl rings are arrayed around the equator of a metal ion. Figure 5 shows the average of the shortest interligand distances between the methyl groups of the pyrazolyl rings (Me···Me). These distances are short, judging from the van der Waals radius of a methyl group (2.0 Å).[32] The average Me···Me distances of the $[B(3\text{-}Mepz)_4]^-$ complexes are shorter than those of the appropriate $[HB(3\text{-}Mepz)_3]^-$ complexes. This is attributable to intraligand contact between the coordinated and non-coordinated pyrazolyl rings. The interligand contact between the methyl groups should increase the strain energy of the complexes.

Figure 6 shows the distribution of the M–N1 distances for all the $[HB(pz)_3]^-$, $[B(pz)_4]^-$, $[HB(3\text{-}Mepz)_3]^-$ and $[B(3\text{-}Mepz)_4]^-$ complexes. The deviations of the M–N1 distances for small metal ions, such as Fe(II), Co(II), Ni(II) and Zn(II), are small in $[HB(pz)_3]^-$ complexes. This suggests that the coordinated pyrazolyl rings in $[HB(pz)_3]^-$ complexes adopt a geometry having high symmetry for small metal ions. The deviations of the M–N1 distances for Cu(II) and the large metal ions, such as Mn(II) and Cd(II), are large in $[HB(pz)_3]^-$ complexes. Because there is a limitation on the distances between the nitrogen atoms of the coordinated pyrazolyl rings (intraligand N1···N1; bite size), the deviations of the M–N1 distances become large for large metal ions. In other words, $[HB(pz)_3]^-$ has less strain and more flexibility in its complexes

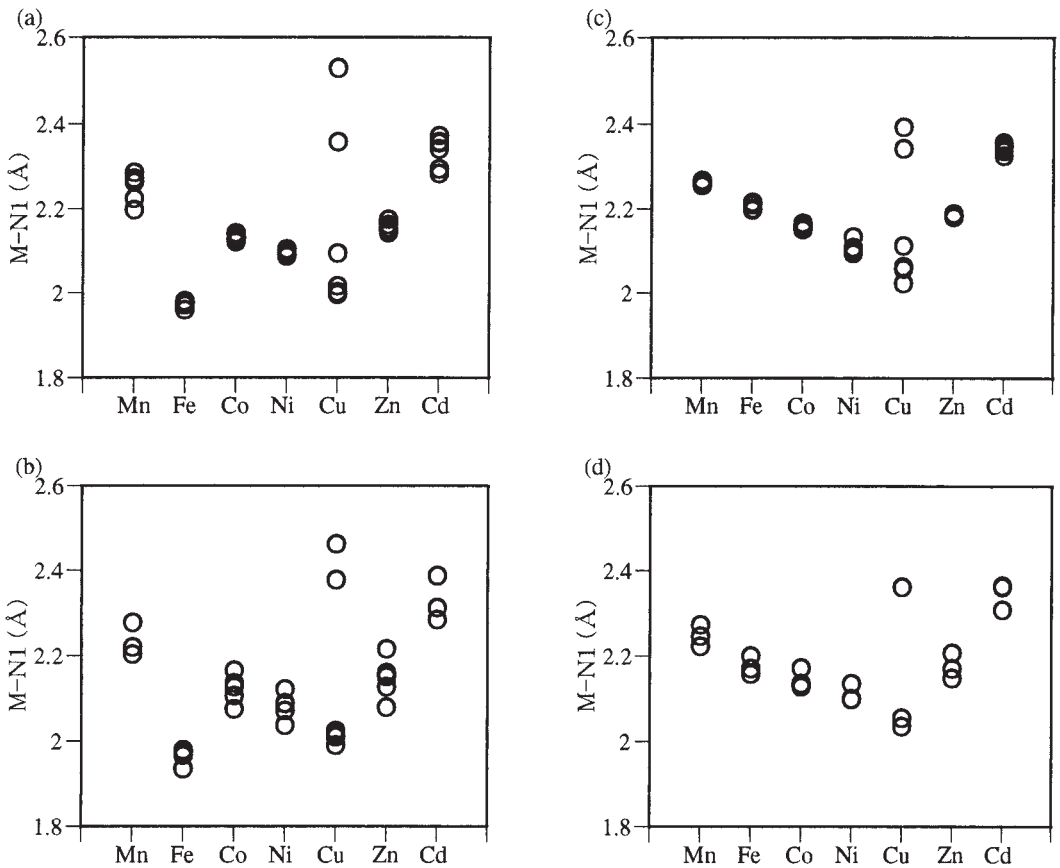

Fig. 6. Distribution of the distances between the metal atom and the coordinated nitrogen atom. Key: (a) $[HB(pz)_3]^-$; (b) $[B(pz)_4]^-$; (c) $[HB(3\text{-}Mepz)_3]^-$; (d) $[B(3\text{-}Mepz)_4]^-$.

than do the other ligands.

The M–N1 distance of $[HB(3\text{-}Mepz)_3]_2Fe$ (**10**) is significantly larger than that of $[HB(pz)_3]_2Fe$. The maximum of the M–N1 distances for Cu(II) in the $[HB(3\text{-}Mepz)_3]^-$ complex (2.39 Å) is smaller than that in $[HB(pz)_3]^-$ (2.53 Å). The deviations of the M–N1 distances are small for $[HB(3\text{-}Mepz)_3]_2Mn$ and $[HB(3\text{-}Mepz)_3]_2Cd$. These are attributable to the interligand contact between the methyl groups of the $[HB(3\text{-}Mepz)_3]^-$ complexes. The interligand contact should decrease the stability of the $[HB(3\text{-}Mepz)_3]^-$ complexes compared to the $[HB(pz)_3]^-$ complexes. This is the reason why all of the studied metal ions were extracted with $[HB(3\text{-}Mepz)_3]^-$ at a substantially higher pH than with $[HB(pz)_3]^-$.

Figure 6 shows that the deviations of the M–N1 distances for small metal ions, such as Fe(II), Co(II), Ni(II) and Zn(II), are large in the $[B(pz)_4]^-$ complexes. This suggests that the intraligand contact between the coordinated pyrazolyl rings and non-coordinated pyrazolyl rings restricts the geometry of the coordinated pyrazolyl rings. Although the M–N1 deviations of the $[B(pz)_4]^-$ complexes for large metal ions, such as Mn(II) and Cd(II), are similar to those of the $[HB(pz)_3]^-$ complexes, the intraligand contact is more severe when the bite size is enlarged.[24] Thus, the stability of the $[B(pz)_4]^-$ complexes for the large metal ions is decreased compared to that of the $[HB(pz)_3]^-$ complexes. Similarly to the situation of $[HB(pz)_3]^-$ and $[B(pz)_4]^-$, the deviations of the M–N1 distances for $[B(3\text{-}Mepz)_4]^-$ are larger than those for $[HB(3\text{-}Mepz)_3]^-$.

The average M–N1 distance of $[B(3\text{-}Mepz)_4]_2Fe$ (**6**) is significantly longer than that of $[B(pz)_4]_2Fe$, and the maximum M–N1 distance for Cu(II) in the $[B(3\text{-}Mepz)_4]^-$ complex is smaller than that in $[B(pz)_4]^-$. In addition, the deviation of M–N1 in the $[B(3\text{-}Mepz)_4]^-$ complexes for small metal ions, such as Co(II), Ni(II) and Zn(II), is smaller than that in the $[B(pz)_4]^-$ complexes. The $[B(3\text{-}Mepz)_4]^-$ complexes experience both the intraligand contact between the coordinated and non-coordinated pyrazolyl rings, and the interligand contact between the methyl groups. The intraligand contact of $[B(3\text{-}Mepz)_4]^-$ enhances the interligand contact between the methyl groups (Fig. 5). This means that the $[B(3\text{-}Mepz)_4]^-$ complexes are the most strained. Thus, all of the studied metal ions are not extracted with $[B(3\text{-}Mepz)_4]^-$ at a lower pH compared to that with $[B(pz)_4]^-$ and $[HB(3\text{-}Mepz)_3]^-$.

Improved Selectivity for Cu(II). As shown in Fig. 5, the average Me···Me distances of the Cu(II) complexes are longer than those of the Co(II) and Ni(II) complexes whose ionic radii are similar to that of Cu(II). In $[HB(3\text{-}Mepz)_3]_2Cu$ (**12**) and $[B(3\text{-}Mepz)_4]_2Cu$ (**13**), the geometry of Cu(II) is a square bipyramid,[27] although that of the other complexes is a trigonally distorted octahedron. Two of the pyrazolyl rings coordinated from the z-axis are further away from the Cu(II) atom than the other coordinated pyrazolyl rings. This geometry relieves the interligand contact in the Cu(II) complexes. Thus, the decrease in the stability of the Cu(II) complexes is smaller than that of the Co(II) and Ni(II) complexes, resulting in an improved selectivity of Cu(II) with $[HB(3\text{-}Mepz)_3]^-$ and $[B(3\text{-}Mepz)_4]^-$.

Decreased Selectivity for Fe(II). The spin state of poly(pyrazolyl)borateiron(II) complexes is an interesting subject. It has been reported that Fe(II) of $[HB(pz)_3]_2Fe$ is spin-crossover state in dichloromethane solution at room temperature,[33] but that it is low-spin state in the crystal.[34] Fe(II) in $[B(pz)_4]_2Fe$ is low-spin state both in a chloroform solution[33] and in the crystal.[35] Judging from the Fe–N1 distances in the crystals of $[HB(3\text{-}Mepz)_3]_2Fe$ (**10**)[25] and $[B(3\text{-}Mepz)_4]_2Fe$ (**6**), Fe(II) is fully high-spin state. Moreover, because ^1H NMR data of **10** and **6** indicated abnormal chemical shifts, Fe(II) is also high-spin state in $CDCl_3$. The variation in the spin state of Fe(II) is controlled by the intra- and interligand contact of the pyrazolyl rings and the methyl groups. Although Fe(II) in $[B(pz)_4]_2Fe$ prefers low-spin state due to the intraligand contact between the coordinated and non-coordinated pyrazolyl rings, Fe(II) in **10** and **6** prefers high-spin state due to the interligand contact between the methyl groups. Since the M–N1 distances of **10** and **6** are longer than those of $[HB(pz)_3]_2Fe$ and $[B(pz)_4]_2Fe$, **10** and **6** are less stable than $[HB(pz)_3]_2Fe$ and $[B(pz)_4]_2Fe$, respectively. Thus, the pH differences in the extraction pH of Fe(II) between the parent ligands and the methyl substituted ligands are larger than those of the other metal ions.

Experimental

General Procedure. $K[HB(3\text{-}Mepz)_3]$ and $K[B(3\text{-}Mepz)_4]$ were synthesized as previously reported.[36,37] All other chemicals were of reagent grade, and distilled water was used throughout. Proton NMR spectra were obtained at 25 ± 1 °C with a JEOL LA-400 spectrometer. Chemical shifts (ppm) were reported downfield from TMS using the solvent $CDCl_3$ ($\delta_H = 7.25$) as an internal standard. The reported ^1H coupling constants are the $^3J_{HH}$ values. The solution was shaken at 25 ± 1 °C with a TAITEC Bio-Shaker BR-30L. The metal ion and ligand concentrations were determined with a Japan Jarrel Ash ICAP-500 inductively coupled argon plasma atomic emission spectrometer or a HITACHI Z-8100 polarized Zeeman atomic absorption spectrometer.

Acid Dissociation and Distribution of $[HB(3\text{-}Mepz)_3]^-$ and $[B(3\text{-}Mepz)_4]^-$. The acid dissociation and distribution constants of the ligands were studied by solvent extraction. An aliquot of chloroform (10 mL) was equilibrated, vigorously with hand, with an equal volume of an aqueous phase containing 1×10^{-1} M of lithium chloride and 1×10^{-3} M of $K[HB(3\text{-}Mepz)_3]$ or $K[B(3\text{-}Mepz)_4]$ buffered with 1×10^{-2} M of sodium acetate, 2-(*N*-morpholino)ethanesulfonic acid (MES), 3-(*N*-morpholino)propanesulfonic acid (MOPS), *N*-tris(hydroxymethyl)methyl-3-aminopropanesulfonic acid (TAPS), 2-(cyclohexylamino)ethanesulfonic acid (CHES), or 3-(cyclohexylamino)propanesulfonic acid (CAPS) at 25 ± 1 °C. After the two phases were separated by centrifugation, the pH of the aqueous phase was measured. The ligand concentration in the aqueous phase was determined from the boron content using ICAP-500. The concentration in the organic phase was measured after back-extraction into 1×10^{-2} M sodium hydroxide.

Extraction of First-Series Transition Metals and Cd(II) Ions. An aliquot of chloroform (10 mL) was shaken with an equal volume of an aqueous phase containing 1×10^{-2} M of $K[HB(3\text{-}Mepz)_3]$ or $K[B(3\text{-}Mepz)_4]$, 1×10^{-4} M of a metal ion and 1×10^{-2} M of acetic acid, MES, MOPS, TAPS, CHES or CAPS at 25 ± 1 °C. After the two phases were separated centrifugally, the pH of the aqueous phase was measured. The metal concentration in the aqueous phase was determined using Z-8100. The concen-

tration in the organic phase was measured after back-extraction into 6 M nitric acid.

Preparation of the Complexes. [HB(3-Mepz)$_3$]$_2$Mn (**1**), [HB(3-Mepz)$_3$]$_2$Co (**2**), [HB(3-Mepz)$_3$]$_2$Zn (**3**), [HB(3-Mepz)$_3$]$_2$Cd (**4**), [B(3-Mepz)$_4$]$_2$Mn (**5**), [B(3-Mepz)$_4$]$_2$Fe (**6**), [B(3-Mepz)$_4$]$_2$Co (**7**), [B(3-Mepz)$_4$]$_2$Ni (**8**) and [B(3-Mepz)$_4$]$_2$Zn (**9**) were prepared in a similar manner to that reported previously.[24] The details of the preparation can be found in Supporting Information. Although Cecchi et al. prepared and characterized **1**–**4**,[26] their X-ray structures have not been reported.

X-ray Crystal Structure Determination. Crystallographic data are summarized in Tables 7 and 8. Crystals of **1**–**9** were each mounted onto a fine glass fiber with epoxy cement. The lattice parameters and intensity data were measured on a Rigaku AFC7R four-circle diffractometer with graphite monochromated Cu Kα radiation ($\lambda = 1.54178$ Å) at 20 ± 1 °C. An ω–2θ scan technique to a maximum 2θ value of 140° was used. An empirical absorption correction based on azimuthal scans of several reflec-

Table 7. Crystallographic Data for [HB(3-Mepz)$_3$]$_2$Mn (**1**), [HB(3-Mepz)$_3$]$_2$Co (**2**), [HB(3-Mepz)$_3$]$_2$Zn (**3**) and [HB(3-Mepz)$_3$]$_2$Cd (**4**)

	1	**2**	**3**	**4**
Chemical formula	$C_{24}H_{32}N_{12}B_2Mn$	$C_{24}H_{32}N_{12}B_2Co$	$C_{24}H_{32}N_{12}B_2Zn$	$C_{24}H_{32}N_{12}B_2Cd$
Formula weight	565.16	569.15	575.60	622.63
Crystal system	triclinic	triclinic	triclinic	triclinic
a/Å	11.122(2)	11.078(2)	11.102(4)	11.172(3)
b/Å	12.626(2)	12.630(2)	12.639(5)	12.638(2)
c/Å	10.763(2)	10.611(2)	10.654(4)	10.891(2)
α/deg	100.43(1)	100.43(1)	100.44(3)	100.40(1)
β/deg	104.72(1)	104.29(1)	104.36(3)	105.05(2)
γ/deg	80.72(1)	81.31(1)	81.16(4)	80.42(1)
U/Å^3	1427.1(4)	1406.1(4)	1415.0(10)	1448.9(5)
T/K	293.2	293.2	293.2	293.2
Space group	$P\bar{1}$ (No. 2)	$P\bar{1}$ (No. 2)	$P\bar{1}$ (No. 2)	$P\bar{1}$ (No. 2)
Z	2	2	2	2
μ(Cu Kα)/mm^{-1}	4.060	5.085	1.502	6.318
Measured reflections	5647	5433	5588	5749
Independent reflections	5347	5137	5296	5436
Observed reflections	4454	3730	4066	4392
Refined parameters	356	356	356	356
$R(F_o)$[a)]	5.75	6.25	4.48	5.27
$wR(F_o)$[b)]	7.85	7.71	6.41	7.10
Goodness of fit	1.91	1.66	1.82	1.75

a) $R(F_o) = \sum(||F_o| - |F_c||)/\sum|F_o|$. b) $wR(F_o) = [\sum w(|F_o| - |F_c|)^2/\sum w|F_o|^2]^{1/2}$.

Table 8. Crystallographic Data for [B(3-Mepz)$_4$]$_2$Mn (**5**), [B(3-Mepz)$_4$]$_2$Fe (**6**), [B(3-Mepz)$_4$]$_2$Co (**7**), [B(3-Mepz)$_4$]$_2$Ni (**8**) and [B(3-Mepz)$_4$]$_2$Zn (**9**)

	5	**6**	**7**	**8**	**9**
Chemical formula	$C_{32}H_{40}N_{16}B_2Mn$	$C_{32}H_{40}N_{16}B_2Fe$	$C_{32}H_{40}N_{16}B_2Co$	$C_{32}H_{40}N_{16}B_2Ni$	$C_{32}H_{40}N_{16}B_2Zn$
Formula weight	725.33	726.24	729.33	729.10	735.78
Crystal system	monoclinic	monoclinic	monoclinic	monoclinic	monoclinic
a/Å	10.183(1)	10.105(1)	10.071(2)	10.042(2)	10.081(3)
b/Å	12.301(1)	12.203(2)	12.164(2)	12.099(2)	12.202(5)
c/Å	14.289(2)	14.260(2)	14.227(2)	14.225(2)	14.257(2)
β/deg	99.45(1)	98.43(1)	97.77(1)	97.25(1)	98.15(2)
U/Å^3	1765.5(4)	1739.4(4)	1726.8(5)	1714.3(4)	1736.0(8)
T/K	293.2	293.2	293.2	293.2	293.2
Space group	$P2_1/c$ (No. 14)	$P2_1/c$ (No. 14)	$P2_1/c$ (No. 14)	$P2_1/c$ (No. 14)	$P2_1/c$ (No. 14)
Z	2	2	2	2	2
μ(Cu Kα)/mm^{-1}	3.442	3.882	4.305	1.226	1.387
Measured reflections	3577	3602	3587	3621	3627
Independent reflections	3387	3460	3397	3422	3425
Observed reflections	2694	2757	2594	2688	2641
Refined parameters	233	233	233	233	233
$R(F_o)$[a)]	4.63	4.90	4.74	5.16	5.17
$wR(F_o)$[b)]	6.87	6.94	5.98	7.89	7.37
Goodness of fit	1.65	1.64	1.48	1.84	1.78

a) $R(F_o) = \sum(||F_o| - |F_c||)/\sum|F_o|$. b) $wR(F_o) = [\sum w(|F_o| - |F_c|)^2/\sum w|F_o|^2]^{1/2}$.

tions was applied to **3**, **8** and **9**, and that using the program DIFABS[38] was applied to the other complexes. The data were corrected for Lorentz and polarization effects, and a correction for secondary extinction was applied. The structures were solved by direct methods[39] and expanded using a Fourier technique.[40] The non-hydrogen atoms were refined anisotropically. Hydrogens were fixed at the positions generated by calculation. All calculations were performed using the teXsan crystallographic software package developed by Molecular Structure Corporation. Crystallographic data have been deposited at the CCDC, 12 Union Road, Cambridge CB2 1EZ, UK and copies can be obtained on request, free of charge, by quoting the publication citation and the deposition numbers 190002–190010 for **1**–**9**, respectively.

References

1 M. Akita, Y. Takahashi, S. Hikichi, and Y. Moro-oka, *Inorg. Chem.*, **40**, 169 (2001).

2 T. Tanase, N. Takeshita, C. Inoue, M. Kato, S. Yano, and K. Sato, *J. Chem. Soc., Dalton Trans.*, **2001**, 2293.

3 M. Rombach and H. Vahrenkamp, *Inorg. Chem.*, **40**, 6144 (2001).

4 U. Brand, M. Rombach, J. Seebacher, and H. Vahrenkamp, *Inorg. Chem.*, **40**, 6151 (2001).

5 M. M. Diaz-Requejo, A. Caballero, T. R. Belderrain, M. C. Nicasio, S. Trofimenko, and P. J. Perez, *J. Am. Chem. Soc.*, **124**, 978 (2002).

6 A. Caballero, F. Gomez-de la Torre, F. A. Jalon, B. R. Manzano, A. M. Rodriguez, S. Trofimenko, and M. P. Sigalas, *J. Chem. Soc., Dalton Trans.*, **2001**, 427.

7 G. R. Motson, O. Mamula, J. C. Jeffery, J. A. McCleverty, M. D. Ward, and A. von Zelewsky, *J. Chem. Soc., Dalton Trans.*, **2001**, 1389.

8 B. S. Hammes, M. W. Carrano, and C. J. Carrano, *J. Chem. Soc., Dalton Trans.*, **2001**, 1448.

9 A. L. Rheingold, L. M. Liable-Sands, and S. Trofimenko, *Inorg. Chem.*, **40**, 6509 (2001).

10 S. Trofimenko, A. L. Rheingold, and L. M. Liable-Sands, *Inorg. Chem.*, **41**, 1889 (2002).

11 A. Beeby, B. P. Burton-Pye, S. Faulkner, G. R. Motson, J. C. Jeffery, J. A. McCleverty, and M. D. Ward, *J. Chem. Soc., Dalton Trans.*, **2002**, 1923.

12 T. J. Crevier, B. K. Bennett, J. D. Soper, J. A. Bowman, A. Dehestani, D. A. Hrovat, S. Lovell, W. Kaminsky, and J. M. Mayer, *J. Am. Chem. Soc.*, **123**, 1059 (2001).

13 J. D. Soper, B. K. Bennett, S. Lovell, and J. M. Mayer, *Inorg. Chem.*, **40**, 1888 (2001).

14 B. K. Bennett, S. J. Pitteri, L. Pilobello, S. Lovell, W. Kaminsky, and J. M. Mayer, *J. Chem. Soc., Dalton Trans.*, **2001**, 3489.

15 E.-S. El-Samanody, K. D. Demadis, T. J. Meyer, and P. S. White, *Inorg. Chem.*, **40**, 3677 (2001).

16 B. C. Brooks, S. H. Meiere, L. A. Friedman, E. H. Carrig, T. B. Gunnoe, and W. D. Harman, *J. Am. Chem. Soc.*, **123**, 3541 (2001).

17 M. T. Valahovic, T. B. Gunnoe, M. Sabat, and W. D. Harman, *J. Am. Chem. Soc.*, **124**, 3309 (2002).

18 K. N. Jayaprakash, T. B. Gunnoe, and P. D. Boyle, *Inorg. Chem.*, **40**, 6481 (2001).

19 D. Conner, K. N. Jayaprakash, T. B. Gunnoe, and P. D. Boyle, *Inorg. Chem.*, **41**, 3042 (2002).

20 N. G. Connelly, D. J. H. Emslie, W. E. Geiger, O. D. Hayward, E. B. Linehan, A. G. Orpen, M. J. Quayle, and P. H. Rieger, *J. Chem. Soc., Dalton Trans.*, **2001**, 670.

21 N. G. Connelly, D. J. H. Emslie, O. D. Hayward, A. G. Orpen, and M. J. Quayle, *J. Chem. Soc., Dalton Trans.*, **2001**, 875.

22 A. E. Enriquez, P. S. White, and J. L. Templeton, *J. Am. Chem. Soc.*, **123**, 4992 (2001).

23 J. Jaffart, M. Etienne, F. Maseras, J. E. McGrady, and O. Eisenstein, *J. Am. Chem. Soc.*, **123**, 6000 (2001).

24 T. Kitano, Y. Sohrin, Y. Hata, H. Kawakami, T. Hori, and K. Ueda, *J. Chem. Soc., Dalton Trans.*, **2001**, 3564.

25 S. Calogero, G. G. Lobbia, P. Cecchi, G. Valle, and J. Friedl, *Polyhedron*, **13**, 87 (1994).

26 P. Cecchi, G. G. Lobbia, F. Marchetti, G. Valle, and S. Calogero, *Polyhedron*, **13**, 2173 (1994).

27 C. Santini, C. Pettinari, M. Pellei, G. G. Lobbia, A. Pifferi, M. Camalli, and A. Mele, *Polyhedron*, **18**, 2255 (1999).

28 D. L. Reger, S. S. Mason, A. L. Rheingold, and R. L. Ostrander, *Inorg. Chem.*, **32**, 5216 (1993).

29 R. D. Shannon, *Acta Crystallogr., Sect. A*, **32**, 751 (1976).

30 F. A. Cotton and G. Wilkinson, ''Advanced Inorganic Chemistry,'' 4th ed, John Wiley and Sons, New York (1980).

31 J. E. Huheey, E. A. Keiter, and R. L. Keiter, ''Inorganic Chemistry,'' 4th ed, Harper Collins, New York (1993).

32 A. Bondi, *J. Phys. Chem.*, **68**, 441 (1964).

33 J. P. Jesson, S. Trofimenko, and D. R. Eaton, *J. Am. Chem. Soc.*, **89**, 3158 (1967).

34 J. D. Oliver, D. F. Mullica, B. B. Hutchinson, and W. O. Milligan, *Inorg. Chem.*, **19**, 165 (1980).

35 Y. Sohrin, H. Kokusen, and M. Matsui, *Inorg. Chem.*, **34**, 3928 (1995).

36 K. Niedenzu, P. M. Niedenzu, and K. R. Warner, *Inorg. Chem.*, **24**, 1604 (1985).

37 S. Trofimenko, ''Scorpionates—The Coordination Chemistry of Poly(pyrazolyl)borate Ligands,'' Imperial College Press, London (1999).

38 N. Walker and D. Stuart, *Acta Crystallogr., Sect. A*, **39**, 158 (1983).

39 A. Altomare, M. C. Burla, M. Camalli, M. Cascarano, C. Giacovazzo, A. Guagliardi, and G. Polidori, *J. Appl. Crystallogr.*, **27**, 435 (1994).

40 P. T. Beurskens, G. Admiraal, G. Beurskens, W. P. Bosman, R. de Gelder, R. Israel, and J. M. M. Smits, ''The DIRDIF-94 program system, Technical Report of the Crystallography Laboratory,'' University of Nijmengen, Netherlands (1994).